Journal of Materials Chemistry C

Accepted Manuscript

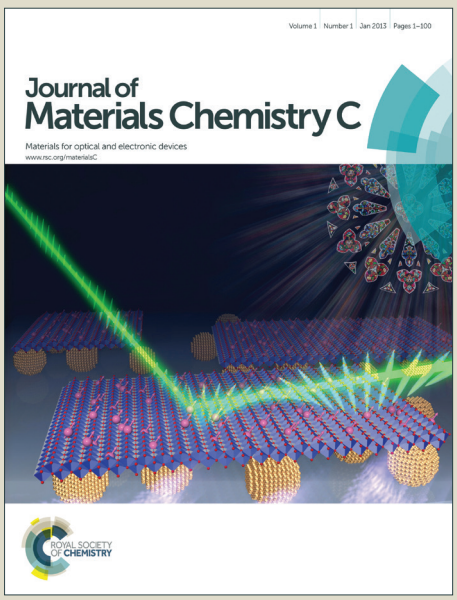

ROYAL SOCIETY OF CHEMISTRY

www.rsc.org/materialsC

Journal Name

RSCPublishing

COMMUNICATION

A Pure Blue Emitter (CIE_y≈0.08) of Chrysene Derivative with High Thermal Stability for OLED

Cite this: DOI: 10.1039/xoxxoooooox

Yao-Hsien Chung,[a] Lei Sheng,[b] Xing Xing,[a] Lingling Zheng,[a] Mengying Bian,[a] Zhijian Chen,[ac] Lixin Xiao,*[ac] and Qihuang Gong[a]

Received ooth January 2012,
Accepted ooth January 2012

DOI: 10.1039/xoxxoooooox

www.rsc.org/

A chrysene derivative BPCC (6,12-bis(9-phenyl-9*H*-carbazol-3-yl)chrysene), possessing high thermal stability with a high glass transition temperature (T_g=181 ℃), was synthesized. Carbazole groups were introduced to improve its hole transporting properties and suppression of crystallization. The device using BPCC as the emitter shows pure saturated blue emission color with coordinates of (0.16, 0.08). Furthermore, utilizing transporting materials with high triplet energy, e.g., TAPC (1,1-bis[4-[N,N-di(p-tolyl)aminophenyl] cyclohexane) and TemPPB (1,2,4,5-tetra(3-pyrid-3-yl-phenyl)benzene) as the hole transport layer (HTL) and electron transport layer (ETL), respectively, the maximum external quantum efficiency (EQE) is 4.9 %. It shows a great potential as highly efficient pure blue emitter for organic light-emitting device (OLED).

Introduction

Although OLED has been commercialized since 1997, a pure blue emitter with high efficiency is still a challenge for full colour display. In addition, we have obtained 100 % internal quantum efficiency of sky-blue electro phosphorescence.[1] Adachi et al. has developed thermally activated delayed fluorescence (TADF) and has achieved 19.5% of EQE with Commission Internationale l'Éclairage (CIE) coordinates of (0.16, 0.20).[2] However, highly efficient, stable deep-blue light with CIEy<0.10 is still under developed. Therefore, many efforts have been paid on highly efficient stable blue fluorescent emitters which can be listed as single-cyclic aromatics;[3] anthracene derivatives;[4] fluorene and spirobifluorenes;[5] polycyclic aromatic hydrocarbons;[6] aromatic amines;[7] nitrogen-containing heterocyclic blue emitters;[8] and other hetero-atom compounds.[9] Among them, anthracene is still the highest efficient emitter, e.g., very recently Kido et al. designed a bisanthracene-based donor-acceptor-type emitter, with an EQE of 10% and CIE coordinates at (0.15, 0.06).[4b]

Considering chrysene as highly efficient component with even higher thermal stability than that of anthracene, however, up to now, no deep blue emission has been achieved. Ionkin et al. reported a tetra-substituted non-fused chrysene, 3,6,9,12-tetrakis(4-*tert*-butylphenyl)chrysene with a radiance of 500 cd m^{-2} at CIE coordinates of (0.23,0.35).[10] Liu et al. synthesized 3,6,9,12-tetra-substituted chrysene with high EQE emission at CIE coordinates of (0.13, 0.20).[11] All the colour purities should be further improved.

In this present, we synthesized a chrysene derivative, BPCC (6,12-bis(9-phenyl-9*H*-carbazol-3-yl)chrysene) with glass transition temperature (T_g = 181 ℃), by introducing carbazole groups to improve its hole transporting property. Moreover, owing to its twist structure resulted from the carbazole group, its crystallization was suppressed and less fluorescence self quenching was expected. We achieved a high EQE of 4.9 % with pure blue emission at CIE coordinates of (0.16, 0.08) by using BPCC as the emitter.

Results and discussion

BPCC was synthesized through Suzuki-Miyaura cross-coupling reaction by 6,12-dibromochrysene with *N*-phenyl-3-carbazole boronate as shown in Scheme 1.

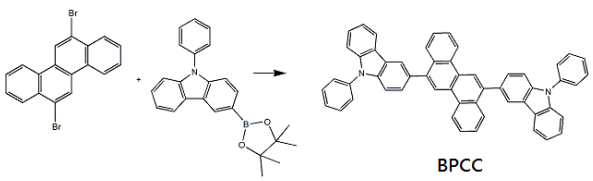

Scheme 1. Synthesis of the chrysene derivative BPCC

The frontier molecular orbital energy levels and the optimized geometries of BPCC are calculated by density functional theory (DFT) with Gaussian program package (Fig. 1). The highest occupied molecular orbital (HOMO) is mainly located at the carbazole moiety and the lowest unoccupied molecular orbital (LUMO) is mainly located at the chrysene moiety. The HOMO and LUMO energy levels for BPCC were calculated to be - 5.4 eV and - 1.6 eV, respectively. According to DFT analysis, the molecular conformation demonstrated that the carbazole at the 6,12-position of chrysene was twisted with a dihedral angle of 57.3 ° respect to the chrysene plane, moreover, the phenyl ring at the 9-position of carbazole was twisted with a dihedral angle of 55.0 ° respect to the carbazole plane. It may suppress molecular aggregation because of

the increased steric hindrance caused by the twisted structure, which is benefit to achieve high efficiency.

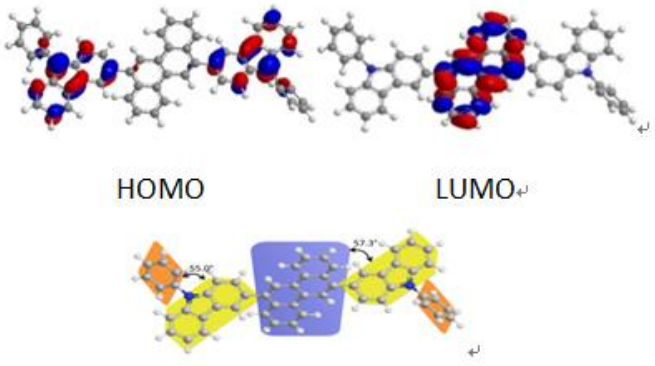

Fig. 1. HOMO LUMO energy level and molecular conformations of BPCC.

The thermal properties of BPCC were measured by differential scanning calorimetry (DSC) and thermogravimetric analysis (TGA). The T_g of BPCC is as high as 181 ℃, the melting point (T_m) and decomposition temperature (T_d) are 342 ℃ and 530 ℃, respectively, indicating high thermal stability.

The absorption and photoluminescence spectra of BPCC in tetrahydrofuran (THF) and thin film were obtained by high-vacuum (10^{-6} torr) thermal evaporation on quartz as shown in Fig. 2

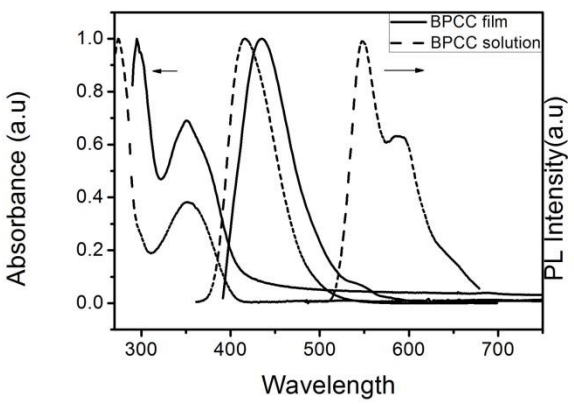

Fig. 2. Absorption, fluorescence and phosphorescence spectra of BPCC.

The absorption of BPCC shows two peaks at 274 and 354 nm in solution, shifting to 295 and 354 nm for the film state. The λ_{max} = 274 nm can be assigned to its π-π* transitions of the molecule. The 354 nm absorption is the characteristic vibration of the chrysene moiety. The emission peak of BPCC in solution is 415 nm, which red shifted to 435 nm for the film state, probably due to its π-π stacking of BPCC molecules. From the absorption edge, their energy band gap can be assumed to be 3.0 eV. According to the HOMO level of 5.6 eV, derived from atmosphere UV photoelectron spectrometer AC-2 (Riken Keiki), its LUMO can be estimated to be as 2.6 eV. The triplet energy is 2.4 eV calculated from the phosphorescence spectrum onset. And the BPCC quantum yield is 0.61 in THF solution with coumarin 151 (Φ: 0.79) as the standard.

To investigate the emitting properties of BPCC, multilayered OLED was fabricated. In order to avoid fluorescent quenching, we optimized the devices by doping BPCC into tCP (20 wt%) as the emission layer. The physical properties of materials were listed in Table 1 and the device structure and energy diagram are shown in Fig 3. To optimize the device structure, we fabricated four deep-blue devices with different charge transporting materials.

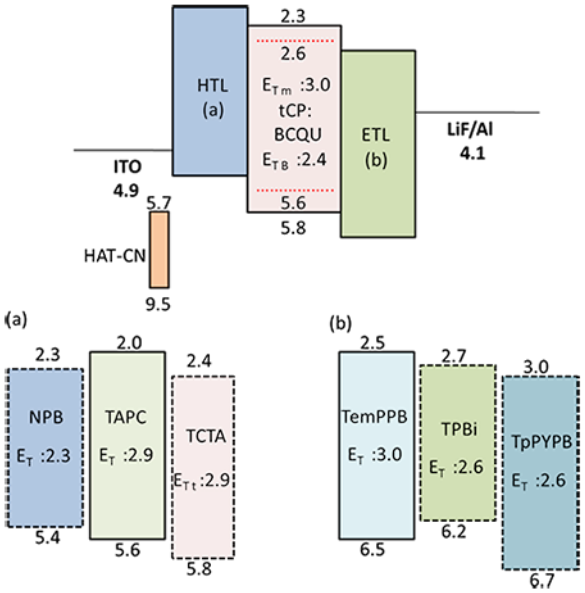

Fig. 3. Energy level diagram in the OLED Devices

Device**A**: ITO/NPB 60 nm/ tCP:BPCC (20 wt%) 10 nm/TPBi 50 nm/LiF 1 nm/Al 100 nm

DeviceB: ITO/TAPC 60 nm/ tCP:BPCC (20 wt%) 10 nm/ TpPYPB 50 nm /LiF 1 nm/Al 100 nm

DeviceC: ITO/TAPC 50 nm /TCTA 10 nm/ tCP:BPCC (20 wt%) 10 nm/TpPYPB 50 nm/LiF1 nm/Al 100 nm

DeviceD: ITO/TAPC 50 nm / tCP:BPCC (20 wt%) 10 nm/TemPPB 50 nm/LiF1 nm/Al 100 nm

Table 1. Physical properties of charge transporting materials used in devices

Material	T_g (°C)	E_a (eV)	I_p (eV)	E_g (eV)	E_T (eV)	Ref
HAT-CN		5.7	9.5	3.8		12
NPB	98	2.3	5.4	3.1	2.4	12
TAPC	78	2.0	5.6	3.6	3.0	13
TCTA	151	2.4	5.8	3.4	2.9	13
TPBi	124	2.7	6.2	3.5	2.6	14
TpPYPB		3.0	6.7	3.7	2.6	15

TemPPB	97	2.5	6.5	4.0	3.0	16
tCP		2.3	5.8	3.5	2.9	17
BPCC	181	2.6	5.6	3.0	2.4	This work

Firstly, we fabricated device **A** using NPB as the hole transporting layer (HTL) and TPBi as electron transporting layer (ETL), these materials can match the energy level of BPCC well. Figure 4 show the current density-voltage and luminous–voltage curves characteristics of BPCC-based device. Figure 5 exhibits the power efficiency (PE) of device **A-D.** The CIE coordinates of device **A** is pretty well at (0.16, 0.10). However, the EQE of device A is only 1.2 %. To improve the efficiency, we designed device **B**, utilizing TAPC with higher hole mobility (1×10^{-2} $cm^{-2}v^{-1}s^{-1}$) than that (5×10^{-4} $cm^{-2}v^{-1}s^{-1}$) of NPB as the HTL, and TpPYPB with higher electron mobility (7.9×10^{-3} $cm^{-2}v^{-1}s^{-1}$)[15] than that (3×10^{-5} $cm^{-2}v^{-1}s^{-1}$) of TPBi as the ETL.

The CIE coordinates of device 1-4**A** are pretty well at (0.16, 0.10) and the full width at half maxima (FWHM) value are around 56 nm (in ESI*). EL spectra and EQE properties of the OLEDs are shown in Figure 6 and EL performances of the OLEDs are summarized in Table 2. However, the EQE of device A is only 1.2 %. To improve the efficiency, we designed device **B**, utilizing TAPC with higher hole mobility (1×10^{-2} $cm^{-2}v^{-1}s^{-1}$) than that (5×10^{-4} $cm^{-2}v^{-1}s^{-1}$) of NPB as the HTL, and TpPYPB with higher electron mobility (7.9×10^{-3} $cm^{-2}v^{-1}s^{-1}$)[15] than that (3×10^{-5} $cm^{-2}v^{-1}s^{-1}$) of TPBi as the ETL.

The turn-on voltage of the device **B** (3.5 V) is lower than device **A** (4.0 V) and the maximum current efficiency (CE) and power efficiency (PE) of device **B** are 2.3 cd A^{-1} and 2.1 lm W^{-1}, respectively, are much higher than that of device **A**, 0.8 cd A^{-1} and 0.5 lm W^{-1} as listed in Table 2. These might be due to the higher mobility of HTL and ETL of device **B** than those of device **A**. Moreover, the HOMO energy level of TAPC is close to that of the host-dopant (tCP), which can improve the hole injection ability. In addition, the layer of TAPC can effectively block electrons due to its high LUMO (2.0 eV) level, and the holes can be effectively blocked by TpPYPB due to its deep HOMO (6.7 eV) level.

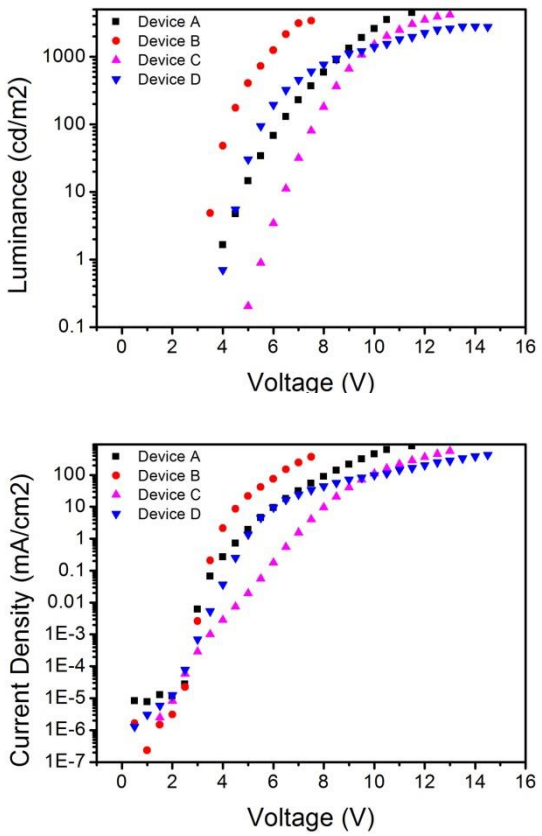

Fig. 4. Current density –voltage and luminous–voltage curves characteristics of BPCC-based device.

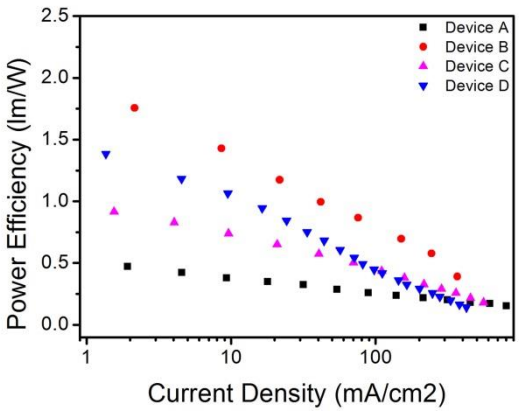

Fig. 5. Power efficiency (PE)-current density curves characteristics of BPCC-based device.

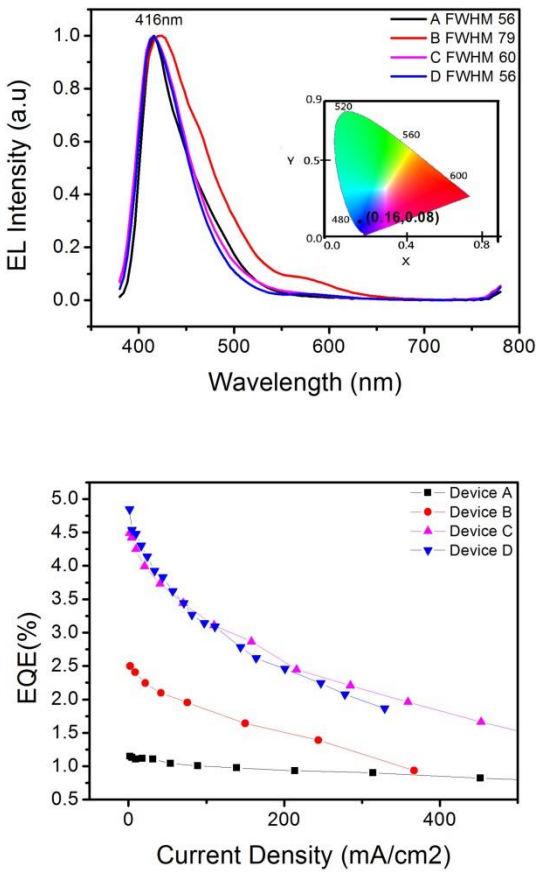

Fig. 6. EL spectra characteristics and EQE-current density of the BPCC-based device.

However, the CIE coordinates of device **B** shift to (0.16, 0.14), which is not saturated pure blue emission. The shifted CIE coordinates of device **B** can be explained by the direct cross recombination transition between electrons and holes trapped on tritolylamine subunits of TAPC molecules[18]. Because the emission layer is only 10 nm, it makes such a pair of trapped carriers much easier. Therefore, we inserted an energy level matched layer of TCTA to suppress excimer formation to fabricate device **C**.

The turn-on voltage of device **C** (5 V) is higher than devices **B** (3.5 V). This might be due to the lower mobility of TCTA than that of TAPC. The brightness of the device is 4150 cd m^{-2}, CIE coordinates shift back to (0.16, 0.08). The EQE achieved 4.5 %.

To reduce the turn-on voltage, we used a weak electron transporting material of TemPPB as previously reported[16] instead of TpPYPB to get device **D**. TemPPB (E_T = 3.0 eV) has super twisted structure property that make it possess higher triplet energy than that of TpPYPB (E_T = 2.6 eV). Although the mobility of TemPPB (3×10^{-7} $cm^{-2}v^{-1}s^{-1}$) is lower than that of TpPYPB, the recombination zone are closer to the layer of TemPPB, which also effectively improve the CIE coordinates and efficiency. Furthermore, the turn on voltage is reducing from 5 V to 4 V. Unexpected, device **D** achieved high EQE of 4.9% with CIE coordinates at (0.16, 0.08), which is very close to the pure blue emission. Although the electron mobility of TemPPB is the lowest, the EQE of device D is the highest. These might be attributed to triplet-triplet annihilation (TTA),[19] resulted from higher triplet energy for both TAPC and TemPPB than those of NPB and TPBi. The electroluminescence spectra of the OLED are shown in Fig. 5. The devices performances are summarized in Table 2.

The devices performances are summarized in Table 2.

Device	Turn-on voltage (V@1cd m^{-2})	Max Luminance (cd m^{-2})	Max *PE*(l m W^{-1})	Max *CE* (cd A^{-1})	Max *EQE* (%)	CIE (x, y)	FWHM (nm)
A	4.0	3342	0.5	0.8	1.2	0.16,0.10	56
B	3.5	3410	2.1	2.3	2.5	0.16,0.14	79
C	5.0	4150	1.0	2.0	4.5	0.16,0.08	60
D	4.0	2790	1.5	2.2	4.9	0.16,0.08	56

Conclusions

In conclusion, a new material BPCC was synthesized based on chrysene group with high thermal stability (T_g=181 °C), carbazole moiety was introduced into the molecule to improve its hole mobility, achieving pure blue with CIE coordinates at (0.16, 0.08). Transporting materials with high triplet energy, e.g., TAPC and TemPPB were used as the HTL and ETL, respectively, to optimize the device structure to achieve 4.9% of EQE. These indicate that BPCC shows a great potential in pure blue organic light emitting device.

Experimental

General

The ^{1}H NMR and C^{13} NMR spectra were recorded on JEOL 270 (270 MHz) spectrometer. Mass spectra were obtained using a JEOL JMS-K9 mass spectrometer. Ultraviolet-visible (UV-vis) absorption, photoluminescence spectra and the FT-IR spectra were recorded on an Agilent UV-vis Spectroscopy System (8453E) and Bruker tensor 27, respectively. The low temperature phosphorescence spectrum measurement was carried out on a HITACHI Fluorescence Spectrometer (F-4600) under liquid nitrogen at 77K.

Differential scanning calorimetry (DSC) was performed on a Perkin-Elmer Diamond DSC Pyris instrument under nitrogen atmosphere at a heating rate of 10 ℃/min. Thermo gravimetric analysis (TGA) was undertaken using a SEIKO EXSTAR 6000 TG/DTA 6200 unit under nitrogen atmosphere at a heating rate of 10 ℃/min. HOMO levels were determined by atmospheric ultraviolet photoelectron spectroscopy (Rikken Keiki AC-2).

Device fabrication

The OLED were fabricated on glass substrates with an indium tin oxide. The substrates were cleaned by deionized water, acetone, ethanol, after the plasma treatments for ten minutes, all of the organic layers were evaporated under 10^{-6} torr. To improve the hole injection from the anode, 1 nm of hexa-aza-triphenylene-hexa-cabonitrile (HAT-CN) was evaporated as the buffer layer, 60 nm of 4,4'-bis[N-(1-naphthyl)-N-phenyl-amino]biphenyl (NPB) or 1,1-bis[4-[N,N-di(p-tolyl)aminophenyl] cyclohexane (TAPC) as the hole transporting material, 10 nm of N,N',N"-1,3,5-tricarbazoloylbenzene (tCP) doped BPCC by weight 20%, 50 nm of 1,3,5-tris(N-phenylbenzimidazol-2-yl)-benzene (TPBi) or 1,3,5-tri(p-pyrid-3-yl-phenyl)benzene (TpPYPB) or 1,2,4,5-tetra(3-pyrid-3-yl-phenyl)benzene (TemPPB) as the electron transporting material. The cathode consisting of 1nm LiF and 100 nm Al was deposited through a shadow mask, with 1 mm^2 for device active area.

Preparation of blue emitters

To a solution of 6, 12-dibromochrysene (1.16 g, 3.0 mmol) and *N*-phenyl-3-carbazole boronate (2.77 g, 7.5 mmol) in THF (20 mL), K_2CO_3 aqueous solution (2M, 20 mL) was added under nitrogen and agitation. Followed by the addition of $Pd(OAc)_2$ (20 mg, 0.6 mmol) and triphenylphosphine (80 mg), the resultant solution was refluxed for 10 hrs. 50 mL water was added to quench the reaction. The solution was concentrated under reduced pressure to remove the organic solvent and then filtered. The residue was washed with deionized water (80 mL), ethanol (80 mL) and ethyl acetate (150 mL) for three times and redissolved in toluene. The crude product was chromatographied on a silica gel and further purified by recrystallization. A white solid was obtained with a yield of 77%. ^{1}H NMR (500MHz, $CDCl_3$): 8.920-8.937 (d, 2H, *J* 8.5 Hz), 8.845 (s, 2H), 8.439-8.441 (d, 2H, *J* 1 Hz), 8.205-8.221 (d, 2H, *J* 8 Hz), 8.153-8.169 (d, 2H, *J* 8 Hz), 7.657-7.722 (m, 12H), 7.541-7.612 (m, 4H), 7.451-7.537 (m, 6H), 7.315-7.346 (m, 2H). ^{13}C NMR (600MHz, $CDCl_3$): δ 141.44, 140.39, 139.77, 137.78, 130.01, 128.46, 127.62, 127.30, 127.20, 126.47, 126.34, 123.55, 122.63, 121.94, 120.53, 120.16, 109.96, 109.57 Anal. calcd for $C_{54}H_{34}N_2$, 710.2716; found, 710.2708. FT-IR (KBr, cm^{-1}): 3045 (s), 1592 (s), 1498 (s), 1456 (s)

Acknowledgements
We acknowledge the financial support from the National Natural Science Foundation of China (61177020 and 11121091) and the National Basic Research Program of China (2013CB328704).

Notes and references
[a] State Key Laboratory for Mesoscopic Physics and Department of Physics, Peking University, Beijing 100871, China
[b] Yantai Valiant Fine Chemicals Co.,Ltd. Shandong 264006, China
[C] New Display Device and System Integration Collaborative Innovation Center of the West Coast of the Taiwan Strait，Fuzhou 350002, China
E-mail: lxxiao@pku.edu.cn;

† Footnotes should appear here. These might include comments relevant to but not central to the matter under discussion, limited experimental and spectral data, and crystallographic data.
1. Electronic Supplementary Information (ESI) available:[Characteristics of doped BPCC-based device 1-4A].

See DOI: 10.1039/b000000x/

1 L. Xiao, S. J. Su, Y. Agata, H. Lan and J. Kido, *Adv.Mater.*, 2009, **21**, 1271.

2 Q. Zhang, B. Li, Huang S, H. Nomura, H. Tanaka and C Adachi, *Nat. Photonics.*, 2014, **8**, 326.

3 C. Hosokawa, H. Higashi, H. Nakamura and T. Kusumoto, *Appl. Phys. Lett.*, 1995, **67**, 3853.

4 (*a*) W. J. Shen, R. Dodda , C. C. Wu, F. I. Wu, T.H. Liu, H.H. Chen, C.H. Chen, and C.F. Shu , *Chem. Mater*., 2004, **16**, 930; (*b*) J. Y Hu, Y. J. Pu, F. Satoh, S. Kawata, H. Katagiri, H. Sasabe and J. Kido, *Adv. Funct. Mater*., 2014, **24**, 2064. (*c*) S. L. Lin, L. H. Chan, R. H. Lee, M. Y. Yen, W. J. Kuo, C. T. Chen and R. J. Jeng, *Adv. Mater*., 2008, **20**, 3947–3952 (*d*) C. H. Chien, C. K. Chen, F-M Hsu, C. F. Shu, P. T. Chou and C. H. Lai, *Adv. Funct. Mater*., 2009, **19**, 560–566(*e*) Y. C. Chang, S. C. Yeh, Y. H. Chena, C. T. Chenc, R. H. Lee and R. J. Jeng, *Dyes Pigments*., 2013, **99**, 577-587

5 (*a*) T. C. Chao, Y. T. Lin, C. Y. Yang, T. S. Hung, H. C. Chou, C. C. Wu and K. T. Wong, *Adv. Mater.*, 2005, **17**, 992; (*b*) Y. Park, J. H. Lee, D. H. Jung, S. H. Liu, Y. H. Lin, L. Y. Chen, C. C. Wu and J. Park., *J. Mater. Chem*., 2010, **20**, 5930; (*c*) C. G. Zhen, Y. F. Dai, W. J. Zeng, Z. Ma, Z. K. Chen, and J. Kieffer, *Adv. Funct. Mater*., 2011, **21**, 699; (*d*) X. Xing, L. X. Xiao, L. Zheng, S. Hu, Z. J. Chen, B. Qu and Q. Gong, *J. Mater. Chem*, **22**, 15136; (*e*) S. K. Kim, B. Yang, Y. Ma, J. H. Lee and J. W. Park, *J. Mater . Chem*., 2008, **18**, 3376.

6 (*a*) B. X. Mi, Z. Q. Gao, C. S. Lee, S. T. Lee, H. L. Kwong, and N. B. Wong, *Appl. Phys. Lett.*, 1999, **75**, 4055; (*b*) H. T. Shih, C. H. Lin and H. H. Shih, *Adv. Mater*., 2002, **14**, 1409; (*c*) K. C. Wu, P. J. Ku, C. S. Lin, H. T. Shih, F. I. Wu, M. J. Huang, J. J. Lin, I. C. Chen and C. H. Cheng, *Adv. Mater*., 2008, **18**, 67.

7 (*a*) Y. Wei and C. T. Chen. *J. Am. Chem. Soc.*, 2007, **129**, 7478; (*b*) H. C. Li, Y. P. Lin, P. T. Chou, Y. M. Cheng and R. S. Liu, *Adv. Funct. Mater*., 2007, **17**, 520; (*c*) M. T. Lee, C. H. Liao, C. H. Tsai and C. H. Chen, *Adv. Mater*., 2005, **17**, 2493.

8 (*a*) S. J. Lee, J. S. Park, K. J. Yoon Y. I. Kim, S. H. Jin, S. K. Kang, Y. S. Gal, S. Kang, J. Y. Lee, J. W. Kang, S. H. Lee, H. D. Park, and J. J. Kim, *Adv. Funct. Mater.* 2008, **18**, 3922; (*b*) C. J. Tonzola, A. P. Kulkarni, A. P. Gifford, W. Kaminsky and S. A. Jenekhe, *Adv. Funct. Mater.*, 2007, **17**, 863.

9 (*a*) H. Y. Chen, W. Y. Lam, J. D. Luo, Y. L. Ho, B. Z. Tang, D. B. Zhu, M. Wong and H. S. Kwok, *Appl. Phys. Lett.*, 2002, **81**, 574; (*b*) M. Zhu and C. Yang, *Chem. Soc. Rev*., 2013, **42**, 4963.

10 A. S Ionkin, W. J. Marshall, B. M. Fish, L. M. Bryman and Y. A. Wang, *Chem. Commun.*, 2008, **20**, 2319 − 2321.

11 T. L. Wu, H. H. Chou, P. Y. Huang, C. H. Cheng and R. S. Liu , *J. Org. Chem.*, 2013, **79**, 267-274.

12 Y.-K. Kim, J. W. Kim, and Y. Park, *Appl. Phys. Lett*., 2009, **94**, 063305

13 S.G. Lee, H Shin, and J.J, Kim, *Adv. Mater*., 2014, **26**, 5863.

14 J. Y. Shen, C. Y. Lee, T.-H. Huang, J. T. Lin, Y.-T. Tao, C.-H. Chien and C. T. Tsai, *J. Mater. Chem*., 2005, **15**, 2455.

15 S. J. Su, T. Chiba, T. Takeda, and J. Kido, *Adv. Mater*., 2008, **20**, 2125.

16 L. Xiao, B. Qi, X. Xing, L. Zheng, K. Sheng, Z. J. Chen, B. Qu, L. Zhang, Z. Ji and Q. Gong, *J. Mater. Chem.*, 2011, **21**, 19058.

17 (*a*) K. S. Son, M. Yahiro, T. Imai, H. Yoshizaki, and C. Adachi, *Chem. Mater*., 2008, **20**, 4439; (*b*) L. Murphy, P. Brulatti, V. Fattori, M Cocchi and J. A. Gareth Williams, *Chem. Commun*., 2012, **48** , 5817.

18 J. Kalinowski, G. Giro, M. Cocchi, V. Fattori and P. Di Marco, *Appl. Phys. Lett.*, 2000, **76**, 2352.

19 Y. J. Pu, G. Nakata, F. Satoh, H. Sasabe, D. Yokoyama and J. Kido, *Adv. Mater*., 2012, **24**, 1765.

